Am. J. Hum. Genet. 69:1033–1045, 2001

Nonmuscle Myosin Heavy Chain IIA Mutations Define a Spectrum of Autosomal Dominant Macrothrombocytopenias: May-Hegglin Anomaly and Fechtner, Sebastian, Epstein, and Alport-Like Syndromes

Karen E. Heath,[1] Angel Campos-Barros,[1,4] Amos Toren,[5] Galit Rozenfeld-Granot,[5] Lena E. Carlsson,[6] Judy Savige,[7] Joyce C. Denison,[8] Martin C. Gregory,[9] James G. White,[10] David F Barker,[8] Andreas Greinacher,[6] Charles J. Epstein,[11] Marc J. Glucksman,[3,12] and John A. Martignetti[1,2]

Departments of [1]Human Genetics and [2]Pediatrics, and the [3]Structural Neurobiology and Proteomics Laboratory, Fishberg Research Center of Neurobiology, Mount Sinai School of Medicine, New York; [4]Department of Pediatric Endocrinology, Hospital Universitario Niño Jesús, Madrid; [5]Department of Pediatric Hemato-Oncology and The Institute of Hematology, The Chaim Sheba Medical Center, Tel-Hashomer, Israel; [6]Department of Immunology and Transfusion Medicine, Ernst-Moritz-Arndt University, Greifswald, Germany; [7]Department of Medicine, Austin and Repatriation Medical Center, University of Melbourne, Heidelberg, Victoria, Australia; [8]Departments of Physiology and [9]Internal Medicine, University of Utah School of Medicine, Salt Lake City; [10]Department of Pediatrics, University of Minnesota, Minneapolis; [11]Department of Pediatrics, University of California, San Francisco; and [12]Department of Biochemistry and Molecular Biology, Finch University of Health Sciences/Chicago Medical School, North Chicago, IL

May-Hegglin anomaly (MHA) and Fechtner (FTNS) and Sebastian (SBS) syndromes are autosomal dominant platelet disorders that share macrothrombocytopenia and characteristic leukocyte inclusions. FTNS has the additional clinical features of nephritis, deafness, and cataracts. Previously, mutations in the *nonmuscle myosin heavy chain 9* gene (*MYH9*), which encodes nonmuscle myosin heavy chain IIA (MYHIIA), were identified in all three disorders. The spectrum of mutations and the genotype-phenotype and structure-function relationships in a large cohort of affected individuals ($n = 27$) has now been examined. Moreover, it is demonstrated that *MYH9* mutations also result in two other FTNS-like macrothrombocytopenia syndromes: Epstein syndrome (EPS) and Alport syndrome with macrothrombocytopenia (APSM). In all five disorders, *MYH9* mutations were identified in 20/27 (74%) affected individuals. Four mutations, R702C, D1424N, E1841K, and R1933X, were most frequent. R702C and R702H mutations were only associated with FTNS, EPS, or APSM, thus defining a region of MYHIIA critical in the combined pathogenesis of macrothrombocytopenia, nephritis, and deafness. The E1841K, D1424N, and R1933X coiled-coil domain mutations were common to both MHA and FTNS. Haplotype analysis using three novel microsatellite markers revealed that three E1841K carriers—one with MHA and two with FTNS—shared a common haplotype around the *MYH9* gene, suggesting a common ancestor. The two new globular-head mutations, K371N and R702H, as well as the recently identified *MYH9* mutation, R705H, which results in DFNA17, were modeled on the basis of X-ray crystallographic data. Altogether, our data suggest that MHA, SBS, FTNS, EPS, and APSM comprise a phenotypic spectrum of disorders, all caused by *MYH9* mutations. On the basis of our genetic analyses, the name "MYHIIA syndrome" is proposed to encompass all of these disorders.

Introduction

Inherited giant-platelet disorders represent a group of rare disorders characterized by thrombocytopenia, large platelets, and variable bleeding symptoms (Mhawech and Saleem 2000). Given lack of reporting and misdiagnosis, the real prevalences of these disorders are most likely underestimated. The autosomal dominant disorders May-Hegglin anomaly (MHA [MIM 155100]; May 1909; Hegglin 1945), Fechtner syndrome (FTNS [MIM 153640]; Peterson et al. 1985), and Sebastian syndrome (SBS [MIM 605249]; Greinacher et al. 1990*b*) share the triad of thrombocytopenia, large platelets, and characteristic leukocyte inclusions (Döhle-like bodies) (table 1). MHA and SBS are differentiated by ultrastructural examination of leukocyte inclusions. These paracrystalline inclusions appear as highly parallel bodies in MHA but are smaller and less organized in SBS and FTNS. FTNS is distinguished by the additional clinical features of high-tone sensorineural deafness, cataracts, and nephritis (Peterson et al. 1985) (table 1). Two other FTNS-like macrothrombocytopenias of unknown genetic etiology have also been described. The first is a subset of auto-

Received June 21, 2001; accepted for publication August 31, 2001; electronically published October 4, 2001.

Address for correspondence and reprints: Dr. John A. Martignetti, Department of Human Genetics, Mount Sinai School of Medicine, Fifth Avenue and 100th Street, Box 1498, New York, NY, 10029. E-mail: john.martignetti@mssm.edu

0002-9297/2001/6905-0012$02.00

Table 1

Clinical and Morphological Features of the Five Autosomal Dominant Macrothrombocytopenias, MHA, SBS, FTNS, EPS, and APSM

	Clinical Feature[a]				
Disorder	MTCP	Leukocyte Inclusions	Nephritis	High-Tone Sensorineural Deafness	Cataracts
MHA	+	+	−	−	−
SBS	+	+	−	−	−
EPS	+	−	+	+	−
FTNS	+	+	+	+	+
APSM	+	−	+	+	+

[a] + = present; − = absent.

somal dominant Alport syndrome (APS), but with platelet defects (APSM [MIM 153650]; Atkin et al. 1986) (table 1). The classic form of APS is an X-linked disorder of the glomerular basement membranes and is characterized by progressive renal failure, deafness, and ocular lesions (MIM 301050; Alport 1927). This form results from mutations in the *COL4A5* gene, which encodes the type IV α-5 collagen chain (Barker et al. 1990). *COL4A5* mutations have not been found in APSM-affected individuals. The second macrothrombocytopenia is Epstein syndrome (EPS [MIM 153650]), which has clinical similarities to FTNS and APSM, although cataracts and leukocyte inclusions have not been described (Epstein et al. 1972) (table 1).

Linkage-analysis studies in families with MHA, FTNS, SBS, and EPS had previously been performed and had localized the disease gene to chromosome 22q11-13 in all disorders (Martignetti et al. 2000; Toren et al. 2000). Subsequently, mutations in the *nonmuscle myosin heavy chain 9* gene (*MYH9*), which lies in this region, were demonstrated in all three disorders: MHA, FTNS, and SBS (May-Hegglin/Fechtner Syndrome Consortium 2000). It has also been shown that a specific missense mutation in *MYH9,* R705H, results in nonsyndromic deafness, DFNA17, an autosomal dominant high-tone sensorineural deafness without platelet abnormalities (Lalwani et al. 2000).

MYH9 encodes nonmuscle myosin IIA (MYHIIA), which is expressed in many different tissues, including platelets, kidney (Simons et al. 1991), leukocytes (Toothaker et al. 1991), and cochlea (Lalwani et al. 2000). Myosins constitute a diverse superfamily, with, to date, 18 different classes. MYHIIA is classified as a class II conventional myosin. These are hexameric enzymes composed of two heavy chains and two pairs of light chains. Dimerization of two heavy chains results in a polar structure with two distinct regions. The amino terminus forms a globular head that binds to actin and ATP, has ATPase activity, and is required for motor activity. The C-terminal α-helical coiled-coil domain comprises the regulatory region (Harrington and Rodgers 1984). Interestingly, mutations in three unconventional myosins have previously been associated with deafness and inner ear hair-cell dysfunction, which is present in FTNS, EPS, and APSM. Mutations in the myosin VIIA gene can result in the Usher syndrome type IB (congenital deafness, vestibular areflexia, and progressive retinitis pigmentosa; Weil et al. 1995) and in recessive nonsyndromic deafness DFNB2 (Liu et al. 1997; Weil et al. 1997). DFNB3 is caused by mutations in the myosin XV gene (Wang et al. 1998). Finally, mutations in the myosin VI gene have been found to result in "*Snell's waltzer*" deafness in mice (Avraham et al. 1995) and, most recently, in a nonsyndromic form of postlingual human deafness, DFNA22 (Melchionda et al. 2001).

In the present study, we performed molecular analyses of 27 previously unstudied families with MHA, SBS, FTNS, EPS, and APSM, defined the common genetic etiology of these five autosomal dominant macrothrombocytopenias, and analyzed structure-function and genotype-phenotype characteristics of detected *MYH9* mutations. Our results, combined with the mutation data of previous studies (Kelley et al. 2000; Lalwani et al. 2000; May-Hegglin/Fechtner Syndrome Consortium 2000 Kunishima et al. 2001), suggest that all six syndromes represent one class of disorder with phenotypic variability. Therefore, the name "MYHIIA syndrome" is proposed to encompass these disorders.

Subjects and Methods

Individuals and Families

After informed consent and institutional review board approval from the corresponding institutions were obtained, blood samples were obtained from 27 individuals with diagnoses of MHA, SBS, FTNS, EPS, and APSM (table 2) and, where possible, from relevant family members. Clinical diagnoses were provided by referring physicians. Urinalysis, ophthalmologic examination, and hearing tests were performed to determine the clinical features of affected individuals. Leukocyte inclusions were characterized by electron microscopy. Genomic DNA was isolated from whole blood (Nicolaides and Stoeckert 1990).

Mutation Analysis

Primers were designed to amplify all 40 coding exons (exons 1–40), their intron/exon boundaries, and regulatory regions (Kawamoto 1994; Beohar and Kawamoto 1998; human *MYH9* GenBank accession number 3135984) (fig. 1 and table 2). PCR amplifications were performed in a 25-μl volume with 10 ng of genomic DNA, 20 μM of each primer, 200 μM dNTPs, 10 mM

Table 2

Clinical and Morphological Features of 27 Individuals with a Diagnosis of MHA, FTNS, SBS, EPS, or APSM

Patient ID Number	Disorder[a]	Ethnic Origin and Country of Origin	Familial or Sporadic	Clinical Feature[b]					Reference for Clinical Details[c]
				MTCP	Döhle-like bodies	Nephritis	Deafness	Cataracts	
1	SBS	European, Germany	Familial	+	+	−	−	−	Greinacher et al. 1990*a*
2	SBS	European, Germany	Familial	+	+	−	−	−	Toren et al. 2000
3	FTNS	European, Germany	ND	+	+	+	+	+	…
4	SBS	European, Germany	Familial	+	+	−	−	−	…
5	MHA/SBS	European, Germany	Familial	+	+	−	−	−	…
6	FTNS	European, U.S.A.	Familial	+	+	−	+	−	…
7	FTNS	African American, U.S.A.	Familial	+	ND	+	+	+	…
8	MHA	European, U.S.A.	ND	+	+	−	−	−	…
9	FTNS	European, U.S.A.	Familial	+	ND	+	+	−	…
10	FTNS	European, U.S.A.	Familial	+	+	−	+	−	…
11	MHA/SBS	European, U.S.A.	Familial	+	+	−	−	−	…
12	FTNS	Iraqi Jewish, Israel	Familial	+	+	+	+	+	Toren et al. 1999
13	FTNS	European, U.S.A.	Familial	+	+	+	+	+	Peterson et al. 1985
14	FTNS	European, Italy	Familial	+	+	+	+	+	Rocca et al. 1993
15	APSM	European, U.S.A.	Familial	+	ND	+	+	−	…
16	EPS	European, U.S.A.	Familial	+	−	+	+	−	Epstein et al. 1972
17	APSM	European, U.S.A.	Sporadic	+	ND	+	−	−	…
18	FTNS	African American, U.S.A.	Sporadic	+	−	+	+	−	Moxey-Mims et al. 1999
19	APSM	European, U.S.A.	Sporadic	+	ND	+	+	−	…
20	APSM	European, U.K.	Sporadic	+	−	+	+	+	…
21	FTNS	European, Italy	Familial	+	+	+	+	−	Velasco et al. 2000
22	EPS	European, U.S.A.	Familial	+	−	+	+	−	Epstein et al. 1972
23	FTNS	European, Belgium	Familial	+	+	+	+	+	…
24	EPS	European, Belgium	Familial	+	−	+	+	−	Nurden and Nurden 1996
25	FTNS	European, Belgium	Familial	+	+	−	+	−	…
26	MHA/SBS	European, Australia	Familial	+	+	−	−	−	…
27	FTNS	Chinese, Australia	Familial	+	+	+	−	−	Colville et al. 2000

Note.—ND = no data available.

[a] Diagnoses of MHA and SBS that were not confirmed by electron microscopy and thus were not differentiated from one another are designated as "MHA/SBS."

[b] + = present; − = absent.

[c] Additional clinical histories are provided in the stated references.

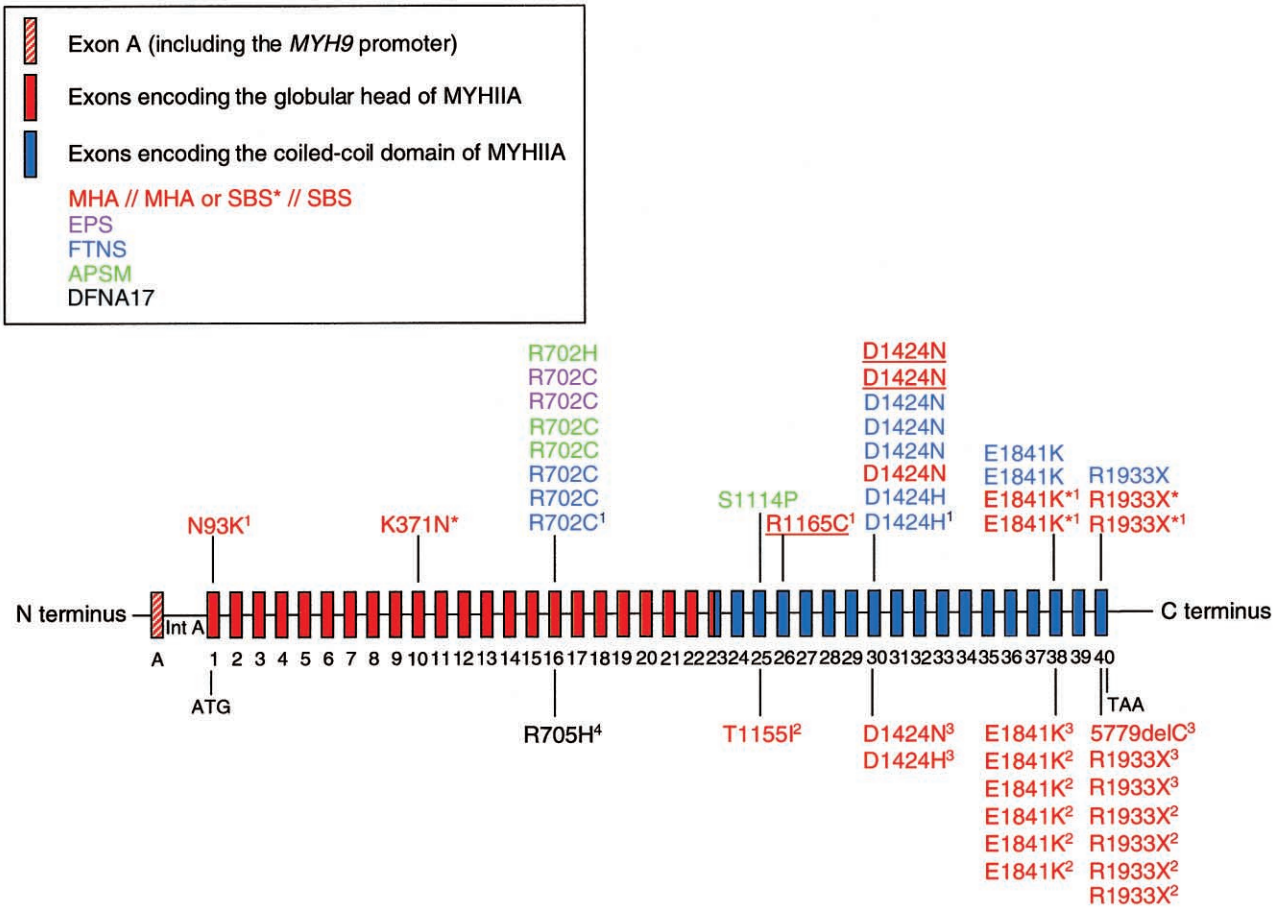

Figure 1 Schematic representation of *MYH9* genomic structure (not drawn to scale) and the spectrum of mutations identified in the *MYH9* gene. The 40 coding exons and the promoter (noncoding exon A) are represented by vertical colored bars. Intron A (Int A) contains enhancer elements. Mutations shown above the genomic structure have been identified in this cohort or in our previous study (May-Hegglin/Fechtner Syndrome Consortium 2000, indicated by a superscript "1"). Mutations shown below the genomic structure have been reported by other groups (Kelly et al. 2000 ["2"]; Kunishima et al. 2001 ["3"]; Lalwani et al. 2000 ["4"]). Clinical disorders are color-coded as shown in the key. Red mutations indicate the purely hematological disorders. Within this group, individuals with MHA are labeled in red, those with SBS are in red and underlined, and those in whom a diagnosis of MHA or SBS could not been differentiated are marked with an asterisk (*).

Tris pH 8.8, 50 mM KCl, 1.5 mM $MgCl_2$, and 0.8 U of Ampli*Taq* GOLD DNA polymerase (Perkin Elmer). PCR cycle conditions included an initial denaturation of 95°C for 10 min, followed by 40 cycles of 95°C for 1 min, 53°C–61°C (table 3) for 1 min, 72°C for 1 min, and a final 5-min extension at 72°C. Amplification of the promoter (see fig. 1) required 5% dimethyl sulfoxide, whereas the exon 31–32 amplimer required 0.4 mM dNTP and an extension time of 2.5 min.

Mutation screening was performed using the Transgenomic Wave denaturing high-performance liquid chromatography (DHPLC) system (Transgenomic). All amplicons were analyzed at two melting temperatures (table 3). Detected heteroduplexes were subsequently sequenced. PCR samples for sequencing were purified (Qiagen) and were sequenced in both directions using ABI BigDye terminator sequencing (Applied Biosystems) on an ABI 3700 DNA Sequencer. Data were analyzed using ABI Sequencing Analysis 3.3 (Applied Biosystems) and Sequencher 3.11 (Gene Codes Corp.) software programs.

DNA sequencing of two independent amplification products confirmed mutations. To rule out polymorphisms, genomic DNA isolated from 94 unrelated control subjects were screened for the presence of the identified mutations, using DHPLC followed by sequencing if any heteroduplex pattern was observed.

Haplotype Analysis

Haplotype analysis was performed to determine the ancestry of certain identified mutations. Four microsatellite markers from the Marshfield Medical Research Foundation and three novel dinucleotide markers, D22S1745, D22S1746, and D22S1747, were analyzed

Table 3

Oligonucleotide Sequences, PCR Annealing Temperature, and DHPLC Conditions for Each *MYH9* Amplicon

MYH9 Amplicon[a]	Oligonucleotide Sequence (5′→3′)		Amplimer Size (bp)	Annealing Temperature (°C)	DHPLC Conditions (starting–final % of solution B [temperature in °C])[b]	
	Sense	Antisense			1	2
Prom	CAG TGG GTG TAG CAG GAA GG	GCG ATG AAG GTG CCA ACT A	395	61	59–65 (68)	59–65 (69)
Enh	CTT AGC CTC CCT GAG CCT CT	CAA AGC CAA AGG GAA ACT CA	211	55	54–60 (61)	54–60 (62)
Ex1	TCC TTC TCC TCC CCG CTT AG	TCC TTC AAG CCC CCT TCT CA	500	55	59–65 (63)	60–66 (61)
Ex2	CAT CAG GGA GTG CCT TCA CA	ATC ACC AGC CAC TAG ATC AA	400	55	60–66 (57)	60–66 (58)
Ex3	CAT CTG TGA CAC TGT GCT CC	GGT TTC AGT AGG AGA CCT CAA G	210	55	54–60 (58)	54–60 (59)
Ex4	ACA CGT TGG GTC CTT CAC G	GTG CTC TTC CTC CAT CAT CCC	284	57	58–64 (62)	58–64 (63)
Ex5	AAA CCT CTG TTC CTG GCA CG	ATA GCA CCG AGT CTG AAC CG	340	55	57–63 (62)	57–63 (64)
Ex6	TGG CCT GGT ACA TGG GTC	AGT GCT GGA ATC AGG AGG CA	302	55	58–64 (59)	58–64 (58)
Ex7	CAT GCC ACT GCA CTC CAA C	TCT TCA GGT GCT CTC CAG C	290	55	55–63 (57)[c]	55–63 (58)[c]
Ex8	ACG TCA CTG GCT ACT CTG CG	CCA CAC TCG ACC ATA GGA GG	320	55	58–64 (61)	58–64 (62)
Ex9	TGG CTT GAG GTG CCT CTG AT	ATT TCC GCA AGA CCT TCC CTC	270	52	55–61 (62)	55–61 (61)
Ex10	TTG CTC ATT CAC CCC GTG G	CCT CAA CTG TGC TGC TGC A	329	55	54–60 (62)	57–63 (59)
Ex11	TTA CTG GGG CAT AGG GTA TGA GG	GGA TAA GGC AAC CAA CAG GC	287	55	56–62 (61)	56–62 (63)
Ex12	TGG GTG GAT AAA GGG AAG GC	AAC CAA CAC AGA GCT GAG GT	430	55	59–65 (61)	59–65 (62)
Ex13	TCT GTG GGA TTC AGG GGA TT	ACT GGG TGA GTC ATT GTG CA	420	55	55–61 (62)	55–61 (63)
Ex14	CTT AGG GGT GGA AAT GCT GGA	ACT GTG GAG GTG GGA AGA TGA	324	55	55–61 (60)	55–61 (62)
Ex15	GGT CCT GTT GTT TCA TTC TGT CTC C	GAG AAA CGA CTG AAG GCT CTG TG	445	55	60–66 (62)	60–66 (63)
Ex16	GTT CCC TGA CTA TTC TCC GAC TG	CAC CTC TGG GAC TCA CTG CA	256	55	53–59 (65)	53–59 (66)
Ex17	CCT TGT CTC ATT CAG CCG AAG A	GCA TCC ACC GAC CAC TGA T	362	55	56–62 (61)	58–64 (57)
Ex18	CCT TCC CAG CAT CCT GTT G	GAA CTG CCC GAT TCT ACT CCT C	697	55	61–67 (62)	63–69 (60)
Ex19	AGC TTG AGG ACA AGA CCA GG	AGC CAG GTA TGT ATG GTG GTG	254	55	56–62 (62)	56–62 (63)
Ex20	TTC CAG CCG AGC ATG TCT CT	CCT GGA CTG AGC CTG CAC TG	210	55	56–62 (61)	56–62 (63)
Ex21	GGC TCT CCA GAT GAA AGC TAC TT	AAA GGG AAC ACC TCT CAC TG	496	55	59–65 (62)	59–65 (63)
Ex22	TGG GCT CAC AGA CCT TGC TA	CAG AAG AGA CAG GAA GCA GC	370	55	59–65 (64)	59–65 (65)
Ex23	GTA CCT CGC TGT TTC AGG GG	AGT GCT GTA GTG TGA CCC AG	450	55	61–67 (59)	61–67 (58)
Ex24	GAG ACA GAA CCC ATG GCA CT	AGT GCC GAG AAC TAG GGC CAG	305	55	57–63 (64)	57–63 (65)
Ex25	TGT CCT GCA AAC TCT GCT CC	TCC ATG TCT CCA AGC CAA GG	350	55	54–60 (62)	54–60 (61)
Ex26	GAA AAG CTG CCT GGA GTG CC	CAG GAC TGG TTT GGA TTC TG	341	55	56–64 (63)[c]	56–64 (62)[c]
Ex27	GGG TCC AGT GAT GAT AGA CC	CAG AGA GCA CAC ATG CAC CT	370	55	61–67 (61)	58–64 (63)
Ex28	TTG TGA CTC AGG TCC AGC TTT	TGC GTG GAC ACA GAG GCC T	260	55	55–61 (63)	55–61 (64)
Ex29	CTA AAT CAG CAG GAC CAG CT	CCT TGA GAG CAC TGA TGT GGG	416	55	58–64 (64)	60–66 (62)
Ex30	$(GGC)_3$TGA GCA GGT GCC ATC TCG G[d]	TCA ACA AGC CAG AGC CTG AG	454	59	54–60 (65)	54–60 (66)
Ex31	TCC CCA GGG AGC TTA GGC	CCG ACC CTC TGT GAT GAC CC	361	59	58–64 (63)	58–64 (62)
Ex32	CCT GAC TTG GGC TCT CTG GG	AGA GAA CAG AAG CCT GCG TG	309	55	57–63 (63)	59–65 (64)
Ex31/32	TCC CCA GGG AGC TTA GGC	ACC CCG AGA CAG GAG GCT A	805	55	63–69 (62)	63–69 (63)
Ex33	CTG AGT TCA GAG CTA GGG CA	TGT AGT TGG CTC AGT CGG GT	290	55	56–62 (63)	56–62 (62)
Ex34	GCA TTG AGT GGA GCA CCA GC	GGA GCC CCG CTA TGA AAC GG	412	55	60–66 (62)	60–66 (61)
Ex35/36	GGG AAG GAT GGT CTT GTG GG	AGG CCA GCT CTG CCG TGG TG	420	55	60–66 (63)	60–66 (64)
Ex37	CCC AAG GGT TTG GTG GGA TC	CTG GTT GTG GCC CAG ATT TG	403	55	60–66 (62)	60–66 (61)
Ex38	CCG GAC CCT CTG AAG GAG G	CCC TGC CTG TCA CCC CAT CT	229	52	55–61 (64)	55–61 (65)
Ex39	AGA TGG GGT GAC AGG CAG GG	GCC AGA AGG GGC AGG GAT TG	401	59	60–66 (62)	60–66 (63)
Ex40	GAG TGG TCC TGT CTA GCT CAG	GGA GGC TGT GGT GTC TGT CT	346	57	57–63 (62)	55–61 (64)

[a] Prom = promoter; Enh = enhancer; Ex = exon.

[b] Solution B consists of 0.1 M triethylammonium acetate (TEAA) and 25% acetonitrile. Time length of gradient was 3 min, unless otherwise specified.

[c] Time length of gradient was 4 min.

[d] $(GGC)_3$ indicates a GC clamp (GGCGGCGGC) placed at the 5′ end of the primer.

(fig. 2). Novel markers were generated. Tandem repeats flanking the *MYH9* gene were identified using the Tandem Repeats Finder program (Benson 1999; Tandem Repeats Finder Web site). The sense and antisense primers (5′→3′), respectively, of the new dinucleotide markers are as follows: D22S1745, CACACACATTTTCTTCATCCAC and CTGGATGAAGTTGGACACC; D22S1746, TTCCCACAGAACCATTCC and CTACTTGAGAATGAGCCACC; and D22S1747, CCTGGAGAGGTCTGAGTATT and GGTCAGGATAAACAGTGGAG. Markers were amplified by PCR in multiplexes, on the basis of their expected sizes and fluorescent end-labels, and then were electrophoretically separated on a 4.2% denaturing polyacrylamide gel, on an ABI 377 DNA Sequencer. Data were analyzed using the ABI Genescan 3.11 and Genotyper 2.5 (Applied Biosystems) software packages. Haplotypes were then determined according to the pedigrees.

Molecular Modeling

The globular-head mutations were modeled onto the X-ray crystallographic structure of the chick smooth-muscle myosin motor domain (Dominguez et al. 1998), obtained from the Protein Data Bank of the Research

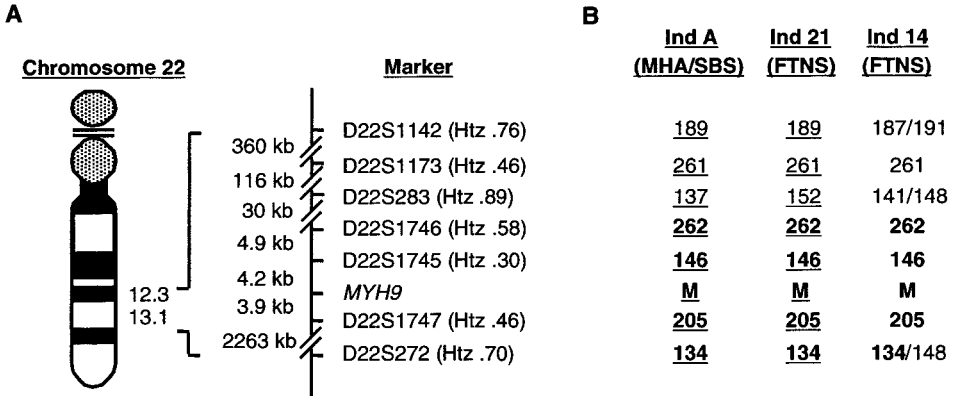

Figure 2 *A,* Chromosome location of *MYH9* and of the microsatellite markers used in the haplotype analysis. Drawing is not to scale. Physical distances are indicated. Heterozygosity (Htz) values for each marker are shown, as determined from the Marshfield Medical Research Foundation human genetic map or by the amplification of DNA from 95 healthy white control individuals (data not shown). *B,* Haplotype analysis of markers flanking the *MYH9* locus in three E1841K carriers. Shared haplotype is indicated in boldface, and genotypes where phase was determined are underlined. M = E1841K mutation. Individual A was reported in our previous study as "individual 3" (May-Hegglin/Fechtner Syndrome Consortium 2000).

Collaboratory for Structural Bioinformatics (ID 1BR2). The atomic coordinates of this structure served as a template for the identified human MYHIIA mutations. All of the amino acids and potentially interacting residues in the chick smooth-muscle myosin were conserved and were identical with respect to the human MYHIIA sequence (fig. 3), and they are numbered according to this sequence. All *in silico* substitutions for the mutations, as well as model building, were calculated and rendered with the computer software suites QUANTA, INSIGHT II (Molecular Simulations), or O (Jones et al. 1991), for molecular visualization. Since no detailed high-resolution structural information is available for the coiled-coil domain, mutations in this region were modeled using helical wheel diagrams (Schiffer and Edmundson 1967).

Results

Spectrum of MYH9 *Mutations*

The 40 *MYH9* coding exons (exons 1–40), the promoter found in exon A, and a 120-bp region of intron A containing enhancer elements (fig. 1) were screened in 27 individuals with a diagnosis of MHA ($n = 4$), SBS ($n = 3$), FTNS ($n = 13$), EPS ($n = 3$), or APSM ($n = 4$), using DHPLC followed by DNA sequencing.

MYH9 mutations were identified for the first time in EPS (R702C) and APSM (R702C, R705H, and S1114P). In total, *MYH9* mutations were identified in 20 affected individuals (table 4). The location of the mutations is represented schematically in figure 1. Eight different single-nucleotide substitutions were identified, including three that were previously undescribed: 1119G→C (K371N) in exon 10, 2105G→A (R702H) in exon 16, and 3340T→C (S1114P) in exon 25 (table 4). Three of the eight mutations were located in the globular head, whereas the remaining five were present in the coiled-coil domain (table 4; fig. 1). Four mutations were frequently observed in this cohort: R702C in exon 16, D1424N in exon 30, E1841K in exon 38, and R1933X in exon 40. The missense mutation R702C was identified in individuals diagnosed with FTNS, EPS, and APSM, whereas the D1424N, E1841K, and R1933X mutations were found in individuals with FTNS, MHA, and SBS (fig. 1).

Several lines of evidence indicated that these mutations were pathological. First, where family members were available, each mutation cosegregated with the respective phenotype. In cases in which the mutation was not present in either parent, it was therefore consistent with a de novo mutation. Second, each of the sequence changes was absent in 94 unaffected, unrelated control individuals. Finally, amino acid sequence-alignment analysis of 15 smooth-muscle and nonmuscle myosins (Sellers 1999, 2000) revealed conservation of the substituted residues (fig. 3) (May-Hegglin/Fechtner Syndrome Consortium 2000).

Evolutionary History of Mutations

To investigate the possible evolution of the mutations, haplotype analysis was performed on the region flanking the *MYH9* locus, using seven microsatellite markers. Four markers previously used for the localization of the gene were used (Martignetti et al. 2000): D22S1142, D22S1173, D22S283, and D22S272 (fig. 2). Three novel markers, D22S1745, D22S1746, and D22S1747 (Ge-

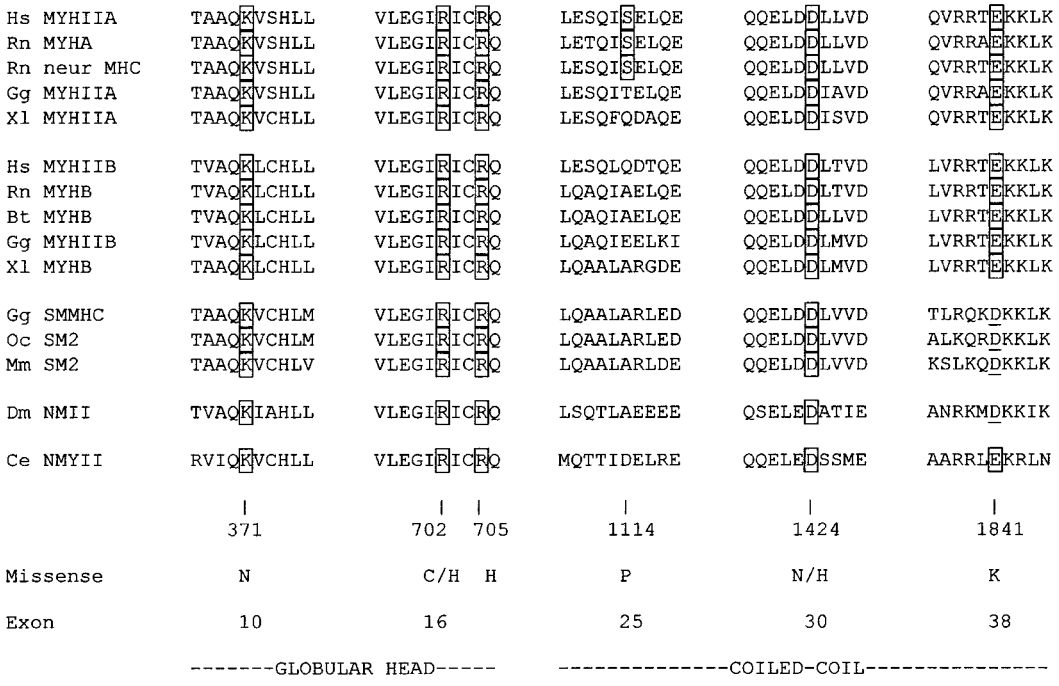

Figure 3 Clustal W alignment of the human MYHIIA amino acid sequence with the amino acid sequences of nonmuscle and smooth-muscle myosins, using the BLASTP program from NCBI. The predicted affected amino acids for the identified missense mutations are shown in boxes. Conserved amino acid changes at the positions of the mutated residues are underlined. Abbreviations and GenBank accession numbers are as follows: Hs MYHIIA, *Homo sapiens* MYHIIA (accession number P35579); Rn MYHA, *Rattus norvegicus* nonmuscle myosin heavy chain A (accession number AAA74950); Rn neur MHC, *R. norvegicus* neuronal myosin heavy chain (accession number S21801); Gg MYHIIA, *Gallus gallus* MYHIIA (accession number AAA48974); Xl MYHIIA, *Xenopus laevis* MYHIIA (accession number AAC83556); Hs MYHIIB, *H. sapiens* MYHIIB (accession number AAA99177); Rn MYHB, *R. norvegicus* nonmuscle myosin heavy chain B (accession number AAF61445); Bt MYHB, *Bos taurus* MYHB (accession number BAA36494); Gg MYHIIB, *G. gallus* MYHIIB (accession number AAA48988); Xl MYHB, *X. laevis* MYHIIB (accession number AAA49915); Gg SMMHC, *G. gallus* SMMHC (accession number P10587); Oc SM2, *Oryctolagus cuniculus* smooth-muscle myosin 2 (accession number P35748); Mm SM2, *Mus musculus* SM2 (accession number JC5421); Dm NMII, *Drosophila melanogaster* nonmuscle myosin heavy chain II (accession number AAB09049); and Ce NMYII, *Caenorhabditis elegans* nonmuscle myosin heavy chain II (accession number AAA83339).

nome Database), were generated against tandem repeat sequences in close proximity to the *MYH9* locus (fig. 2). D22S1745 and D22S1746 lie ~4.2 kb and ~9.1 kb centromeric (3′) to the *MYH9* gene, respectively, and D22S1747 is positioned ~3.9 kb telomeric (5′) to the *MYH9* gene (fig. 2). Genomic DNA from >100 white individuals was amplified for each marker. The heterozygosity values for these novel markers were .36, .58, and .46, respectively, and the number of observed alleles was 6, 13, and 6, respectively (see the Genome Database Web site). Using these seven markers, haplotypes were determined for seven R702C carriers, two families with D1424N, and three E1841K carriers (two families and one individual) from this cohort (table 4) and our previous study (May-Hegglin/Fechtner Syndrome Consortium 2000). Phase was determined, where possible, in two families with the D1424N mutation (FTNS individuals 9 and 23) and in two E1841K carriers: individual 21 (with FTNS) in this cohort and one individual (with MHA/SBS) from our previous study (May-Hegglin/Fechtner Syndrome Consortium 2000). The phase was indeterminable in the third E1841K carrier (individual 14), and a possible disease haplotype was constructed from the alleles present at each genotype. A common haplotype was demonstrated for three E1841K carriers (fig 2). No common haplotype was demonstrated for the R702C or D1424N carriers (data not shown).

Molecular Modeling

The MYHIIA globular-head mutations K371N and R702H, first described in this cohort, as well as the R705H mutation identified in nonsyndromic deafness, DFNA17 (Lalwani et al. 2000), were modeled on the X-ray crystallographic structure of chick smooth-muscle myosin (fig. 4) (Dominguez et al. 1998). Each of the specific residues is invariant within known nonmuscle myosins and the chick smooth-muscle myosin heavy chain (SMMHC) (fig. 3).

The R702H and R705H mutations lie within or ad-

Table 4

***MYH9* Mutations Identified in the Cohort of 27 Individuals with a Diagnosis of MHA, FTNS, SBS, EPS, or APSM, as Indicated**

Patient ID Number[a]	Disorder	Ethnic Origin and Country of Origin	Exon	Nucleotide Substitution (Codon Change)	Protein Alteration	MYHIIA Domain
1	SBS	European, Germany	30	4270G→A (GAC→AAC)	D1424N	Coiled coil
2	SBS	European, Germany	30	4270G→A (GAC→AAC)	D1424N	Coiled coil
3	FTNS	European, Germany	16	2104C→T (CGT→TGT)	R702C	Globular head
5	MHA/SBS	European, Germany	10	1119G→C (AAG→AAC)	K371N[b]	Globular head
8	MHA	European, U.S.A.	30	4270G→A (GAC→AAC)	D1424N	Coiled coil
9	FTNS	European, U.S.A.	30	4270G→A (GAC→AAC)	D1424N	Coiled coil
10	FTNS	European, U.S.A.	30	4270G→C (GAC→CAC)	D1424H	Coiled coil
13	FTNS	European, U.S.A.	30	4270G→A (GAC→AAC)	D1424N	Coiled coil
14	FTNS	European, Italy	38	5521G→A (GAG→AAG)	E1841K	Coiled coil
15	APMS	European, U.S.A.	16	2105G→A (CGT→CAT)	R702H[b]	Globular head
16	EPS	European, U.S.A.	16	2104C→T (CGT→TGT)	R702C	Globular head
17	APSM	European, U.S.A.	25	3340T→C (TCT→CCT)	S1114P[b]	Coiled coil
18	FTNS	African American, U.S.A.	16	2104C→T (CGT→TGT)	R702C	Globular head
19	APSM	European, U.S.A.	16	2104C→T (CGT→TGT)	R702C	Globular head
20	APSM	European, U.K.	16	2104C→T (CGT→TGT)	R702C	Globular head
21	FTNS	European, Spain	38	5521G→A (GAG→AAG)	E1841K	Coiled coil
22	EPS	European, U.S.A.	16	2104C→T (CGT→TGT)	R702C	Globular head
23	FTNS	European, U.S.A.	30	4270G→A (GAC→AAC)	D1424N	Coiled coil
26	MHA/SBS	European, Australia	40	5797C→T (CGA→TGA)	R1933X	Coiled coil
27	FTNS	Chinese, Australia	40	5797C→T (CGA→TGA)	R1933X	Coiled coil

[a] Patient IDs are the same as those listed in table 2.
[b] Previously undescribed mutation.

jacent to the "SH1-SH2" helix of the globular-head domain, proximal to the highly reactive "SH1" cysteine that is responsible for the power transduction state. On the basis of predictions from the wild-type chick SMMHC crystallographic structure, the δ-guanido groups of the two wild-type arginines supply positive charge density within the overall negatively charged cleft (fig. 4*b*). The introduction of a histidine residue at position 702 (fig. 4*a* and 4*c*) would reduce the positive charge density. The wild-type arginine at position 705 can form potential stabilizing interactions with either L89 or A87 (fig. 4*d*). The mutation to H705 disrupts the potential bonding pattern, preventing these stabilizing interactions (fig. 4*e*).

K371 resides in the middle of an α-helix (fig. 4*f*). The potentially reactive ϵ-amino group of the wild-type lysine residue is oriented perpendicular to the axis of the helix, facing towards the solvent and completely exposed, with no apparent interactions with other portions of the protein (fig. 4*f*). The K371N mutation results in the potential creation of a bond between the amide nitrogen of the asparagine and the carbonyl oxygen of the T367 residue at the n-4 position in the α-helix (fig. 4*g*). Thus, this mutation could result in the abnormal stabilization of the region.

Helical wheel representations (Schiffer and Edmundson 1967) were used to assess the possible altered interactions resulting from the S1114P and D1424N mutations in the coiled-coil domain (data not shown). Although the serine residue is only conserved in the myosin IIA subclass, a change to proline would be expected to have a major effect on the α-helical secondary structure, since it is a classical α-helix "breaker" and thus could alter coiled-coil interactions. The other amino acids found at this position within the myosin family are compatible with the maintenance of an α-helical conformation. Most notably, the conserved α-helical domain, ~1,100 amino acids in length, contains no other prolines. The D1424N mutation involves the change to the amide form of the wild-type residue. Although there is no drastic change in the side group conformation, a loss of a potentially favorable coulombic interaction occurs in a structurally critical position, as suggested by conservation of this residue (May-Hegglin/Fechtner Syndrome Consortium 2000) (fig. 3).

Discussion

In the present study, the spectrum of *MYH9* mutations and the genotype-phenotype relationship in 27 individuals diagnosed with MHA, SBS, FTNS, and two FTNS-like disorders—EPS and APSM—were investigated. The combination of previously identified mutations, *MYH9* mutations reported here, and haplotype data indicates that MHA, SBS, FTNS, APSM, and EPS represent a class of allelic disorders with variable phenotypic diversity. This spectrum of disorders is collectively being termed "MYHIIA syndrome."

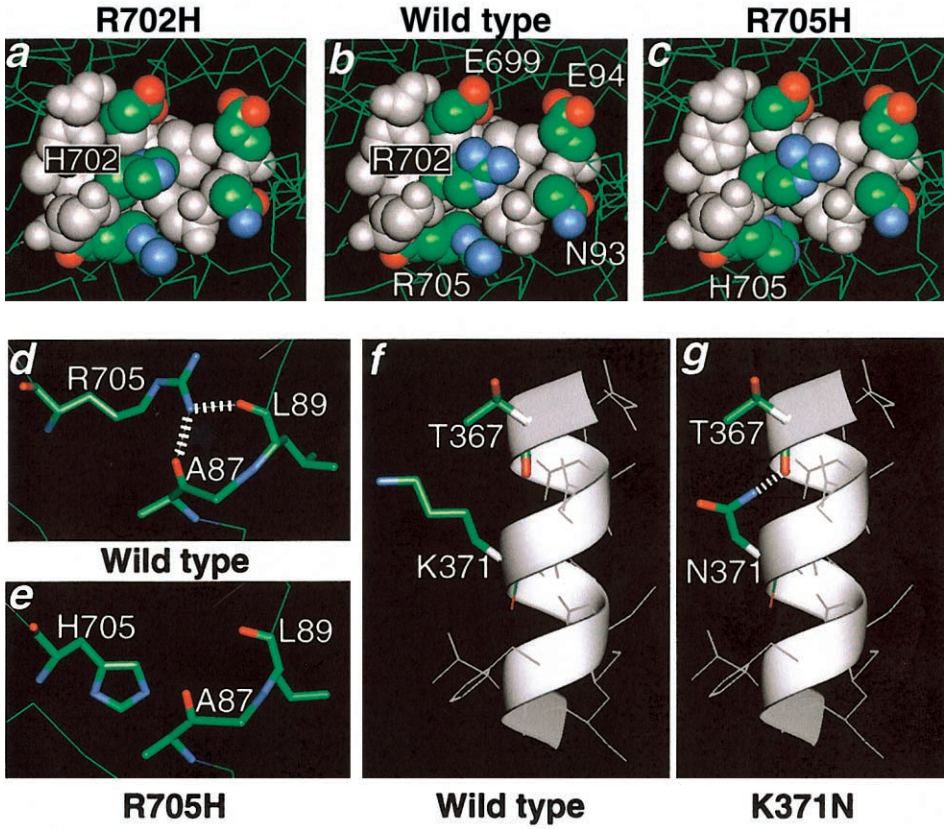

Figure 4 A space-filling representation of the wild-type chick smooth-muscle myosin (*b*) compared with the mutated residues R702H (*a*) and R705H (*c*); This 4.5-Å radial sphere was derived from the X-ray crystallographic structure (Dominguez et al. 1998), as described in the Subjects and Methods section. *d*, Possible interactions of wild type. *e*, Ablation of these interactions in the R705H mutation. *f*, Alpha helical conformation of wild type. *g*, Potential stabilization of mutation K371N.

Mutation Analysis

Eight different mutations in the *MYH9* gene were identified in this new group of affected families, including three that were previously undescribed: K371N, R702H, and S1114P. The R702C mutation, previously identified in patients with FTNS, has now also been identified in patients with EPS and APSM, suggesting that *MYH9* mutations can also be the cause of these two disorders. Moreover, the clinical phenotype of FTNS, APSM, and EPS, as well as our genetic data, suggest that all three conditions are, in fact, the same disease entity.

Our data reveal the presence of frequent mutations within this spectrum of clinically and morphologically distinguishable macrothrombocytopenias. This is more apparent when our data are combined with all reported mutations (fig. 1; Kelley et al. 2000; May-Hegglin/Fechtner Syndrome Consortium 2000; Kunishima et al. 2001). The mutation-detection rate for MYHIIA syndrome was 74% (20/27). If each phenotypic variation is taken into consideration, the mutation-detection rates were as follows: MHA/SBS, 71% (5/7); FTNS (including APSM), 76% (13/17); and EPS, 67% (2/3).

Genotype-Phenotype Correlations

The clinical phenotype of individuals sharing the same mutation can be variable, as is demonstrated by individuals with the D1424N, E1841K, and R1933X mutations. First, the D1424N mutation in exon 30, previously described in only one patient with MHA (Kunishima et al. 2001), was detected in an additional patient with MHA (individual 8), and now in individuals with FTNS (individuals 9, 13, and 23) and SBS (individuals 1 and 2). Second, the E1841K mutation in exon 38, previously described in patients with MHA and MHA/SBS (Kelley et al. 2000; May-Hegglin/Fechtner Syndrome Consortium 2000), has now been found in two patients with FTNS, individuals 14 and 21. Third, the exon 40 missense mutation, R1933X, previously found in a large Italian family with MHA and originally used for linkage of this trait (Martignetti et al. 2000;

May-Hegglin/Fechtner Syndrome Consortium 2000), has now been identified in an additional seven patients with MHA: individual 26 of the present study, four individuals reported by Kelley et al. (2000), and two individuals reported by Kunishima et al. (2001), as well as in a patient with FTNS (individual 27 of the present study). Thus, all three mutations have been found in patients with FTNS and MHA/SBS.

Finally, the R702C mutation in exon 16 has now been shown to occur in a total of eight individuals with a diagnosis of FTNS, EPS, or APSM. Since these three disorders share the clinical features of macrothrombocytopenia, deafness, and nephritis, the genetics suggest that all three disorders may be classified as one syndrome with mild phenotypic variation, including the presence/absence of presenile cataracts. Moreover, a different mutation at the same codon, R702H, was identified in individual 15, who was also diagnosed with APSM. In marked contrast, no mutations have been found in this codon in the purely hematological disorders, MHA and SBS ($n = 7$). Therefore, substitutions at codon 702 are consistently associated with the manifestation of nephritis and deafness in addition to macrothrombocytopenia, indicating that the preservation of codon 702 is critical for the maintenance of MYHIIA function in these affected organs.

A different mutation located in the same region, R705H, was recently identified in a family with nonsyndromic deafness, DFNA17 (Lalwani et al. 2000). Interestingly no platelet abnormalities, leukocyte inclusions, nephritis, or cataracts were observed in any of the family members (Lalwani et al. 2000). Thus, the mutations in these two codons, R702C, R702H, and R705H, appear to define a common region associated with the pathogenesis of deafness, whereas codon 702 seems specifically involved in the molecular pathology of macrothrombocytopenia and nephritis.

Structure-Function Relationships

Previously, six MYHIIA mutations (May-Hegglin/Fechtner Syndrome Consortium 2000) with structure-function correlates were revealed, according to structural data derived from the molecular modeling of the chick smooth-muscle X-ray crystallographic structure (Dominguez et al. 1998) for the N-terminal globular-head mutations and from helical wheel analysis for the carboxy-terminal coiled-domain α-helical mutations. The R702C mutation occurs in the "SH1-SH2" helix that links the interface of the converter domain with the amino terminus of the myosin head. There are two highly reactive cysteine residues at either end of this "SH1-SH2" helix, C694 and C704, which are critical to the conformational changes of the globular-head domain accompanying specific states of power transduction in the myosin-ATPase system (Harrington and Rodgers 1984). Additionally, this region has been implicated in the "swinging lever arm" hypothesis to explain the structural basis of motility (reviewed by Houdusse and Sweeney [2001]).

Two additional mutations lying in this region of MYHIIA—R702H (individual 15) and R705H (Lalwani et al. 2000)—were analyzed. The R702H and R705H mutations share several common structural features. Both residues are present in α-helices of the "SH1-SH2" region (Dominguez et al. 1998) and involve the alteration of basic amino acid residues, which are among the most energetically favorable and stabilizing side chains in α-helices. Judging from amino acid substitutions on a well-characterized synthetic peptide that forms an α-helical polypeptide (O'Neil and DeGrado 1990), the mutations to histidine at both the R702 and R705 positions would result in an energy difference of 0.62 kcal/mole in the α-helix, thus destabilizing the secondary structure. Myosin cross-linking studies have biochemically confirmed these potential interactions and the close proximity of the residues within the domain depicted in figure 4*a* and *c* (Lu and Wong 1989). Lastly, modifications in the region of the two cysteines defining the functionality of this helical region have been shown to have severe biochemical ramifications, by altering nucleotide exchange, ATPase activity, and actin sliding activity (Tiepold et al. 2000). In addition to the destabilizing forces of the R→H mutations within this helical region, the R705H mutation involves the disruption of potential bonds with A87 or L90, resulting in a lower propensity for stability of this secondary structure motif (fig. 4*e*).

The S1114P mutation present in individual 17 is expected to result in a highly unstable protein. Energy calculations using a synthetic peptide show that the replacement of a serine with a proline greatly destabilizes the helix, by >2.65 kcal/mol (O'Neil and DeGrado 1990). It is interesting to note that, in accord with the structural constraints imposed by proline, no proline residues are present in the wild-type MYHIIA coiled-coil domain. This ~1,100–amino acid sequence stretches from the end of the head domain (P836) to within 33 amino acids of the carboxy terminus (P1927, P1931, and P1958).

Unexpectedly, and in contrast to the aforementioned changes, the previously undescribed globular-head mutation K371N in individual 5 (fig. 4*g*) results in an apparent stabilization of the region, by the creation of a bond between the amide nitrogen of the asparagine with the carbonyl oxygen of the T367 residue at the n-4 position in this exposed surface α-helix.

Three of the five missense mutations present in the coiled-coil domain, D1424H, E1841K, and R1933X, were described in the first study (May-Hegglin/Fechtner Syndrome Consortium 2000). These coiled-coil domain

mutations cannot be directly modeled onto homologous structures that are solved to atomic resolution by current structural biological approaches. The common D1424N mutation resides in a region of the α-helical coiled coil, producing a higher-ordered left-handed superhelix. This is an energetically feasible way of stabilizing the long helix at the carboxy terminus. Electrostatic interactions of residues surrounding the hydrophobic interface of the coiled coils provide further stabilization of the chains. Although the change of an aspartic acid to its corresponding nonionizable amide asparagine is a relatively conservative alteration, with respect to the possible interacting surface areas and three-dimensional space-filling conformation, the examination of this mutation through use of a helical wheel diagram indicates a potential destabilizing effect. A net change in the charge density (-1 to 0) may destabilize the interaction, with concomitant deleterious effects upon the normal protein dimerization and assembly in that portion of the α-helical coiled coil.

Haplotype Analysis

The haplotype analysis indicated a common haplotype at a minimal distance of 2.3 Mb surrounding the *MYH9* locus (D221746 to D22S272) in the three E1841K carriers. Similar analyses suggested multiple origins of the R702C and D1424N mutations. One of the three E1841K carriers had a clinical diagnosis of MHA/SBS (May-Hegglin/Fechtner Syndrome Consortium 2000), whereas two had FTNS (individuals 14 and 21). These two individuals had nephritis and deafness, although only individual 14 had cataracts. Further clinical and historical investigation of the family with MHA/SBS confirmed the absence of nephritis, deafness, and ocular abnormalities. The allele frequencies of the four markers that form the shared haplotype were determined in a white control population or were taken from the CEPH database. Given the frequency of the shared alleles, the probability of three unrelated individuals sharing this haplotype was calculated to be <1 in 2×10^6. Therefore, these three families may share a common ancestor. Thus, it is hypothesized that MHA/SBS and FTNS are phenotypic variations of a single syndrome. This could explain why intrafamilial phenotypic variation occurs in these disorders, as observed by us and others (Peterson et al. 1985; Rocca et al. 1993).

Conclusion

Mutations were not identified in all affected individuals (7/27). The absence of a mutation may be explained both at the clinical and molecular level. Macrothrombocytopenia is a genetically heterogeneous disorder (Mhawech and Saleem 2000). In addition, there is a normal distribution of platelet size, ranging from very small to giant (Bain 1985). The combination of macrothrombocytopenia, leukocyte inclusions, and the additional phenotypic features of nephritis, deafness, and cataracts are unique to FTNS, EPS (no cataracts), or APSM and thus are more "readily diagnosed" as a single syndrome entity. MHA and SBS are diagnosed on the basis of the presence of macrothrombocytopenia and Döhle-like bodies, as well as from the pattern of inheritance. Döhle-like bodies are generally visible only if a blood smear is stained with May-Grünwald Giemsa stain in a time-dependent manner (Greinacher et al. 1990*a*, 1992). Ultrastructural features of these inclusions are only detectable by electron microscopy, and this preparation is also time sensitive. Thus, the diagnosis may either be missed or incorrectly applied, depending on the availability of appropriate testing facilities.

At the molecular level, a mutation in *MYH9* may not have been identified for different reasons. First, because of technical limitations: DHPLC has been shown to be a highly sensitive mutation-detection technique (Choy et al. 1999), but, as with any screening strategy, mutations may still be missed. Second, the mutation may be present outside the analyzed regions—for example, in a noncoding region that may have a regulatory function. Third, the mutation may be a deletion or duplication on the order of a single exon, which would be undetected by DHPLC and DNA sequencing, or the mutation could be a major deletion or duplication that would only be detected by northern or Southern analysis. Finally, since *MYH9* mutations were identified in 74% of individuals, genetic heterogeneity cannot be excluded. Mutations may be present in the associated myosin light chains, in another nonmuscle myosin, or in a protein that forms complexes with MYHIIA.

In summary, *MYH9* mutations in patients with EPS and APSM, as well as additional *MYH9* mutations in patients with MHA, FTNS, and SBS, have been identified. These mutations occurred in conserved positions and critical regions in both the globular-head and the coiled-coil domains of MYHIIA and are therefore predicted to result in altered assembly, dimerization, or stability of the quaternary myosin complex. Whether the molecular pathogenesis of these disorders arises from a dominant-negative effect caused by the formation of normal-defective myosin dimers or by haploinsufficiency is currently under investigation. The causes of the phenotypic variation also remain to be delineated. For example, a gene-modifier effect (reviewed by Nadeau [2001]) could be present. A second possibility is the involvement of a regulatory factor that affects the differential expression of *MYH9* in the affected tissues. Altogether, the molecular and clinical data indicate that these six disorders—MHA, SBS, FTNS, EPS, APSM, and DFNA17—represent variants of a single syndrome,

MYHIIA syndrome, with a broad phenotypic spectrum ranging from a lack of symptoms, mild bleeding tendencies, or high-tone sensorineural deafness to severe macrothrombocytopenia with deafness, presenile cataracts, and nephritis, resulting in end-stage renal failure.

Acknowledgments

The authors thank the families and individuals for participation in this study, as well as their referring physicians and scientists: N. Bizzaro, Simon Davies, M. Espinosa, Barbara Greenbaum, Jeffrey Hord, Naomi Luban, Jenny Kim, Eric Legius, Gert Matthijs, Alan Nurden, Chris Van Geet, Lionel van Maldergen, and D. Velasco. We also thank Maria Ramirez and Dan Musat, for their technical assistance, and I. Visiers, for discussion. This work represents partial fulfillment of the Ph.D. requirements for A.T., at the Sackler Faculty of Medicine, Tel Aviv University. K.E.H. was funded, in part, by the Charles H. Revson Foundation; A.C.B. was funded, in part, by Spanish Ministry of Health grant FIS 00/3145; and J.A.M. was supported with grant 5 P30 HD28822 from the Mount Sinai Child Health Research Center.

Electronic-Database Information

Accession numbers and URLs for data in this article are as follows:

Center for Medical Genetics, Marshfield Medical Research Foundation, http://research.marshfieldclinic.org/genetics/ (for the human genetic map)

GenBank, http://www.ncbi.nlm.nih.gov/Genbank/ (for human *MYH9* [accession number 3135984], Hs MYHIIA [accession number P35579], Rn MYHA [accession number AAA74950], Rn neur MHC [accession number S21801], Gg MYHIIA [AAA48974], Xl MYHIIA [accession number AAC83556], Hs MYHIIB [accession number AAA99177], Rn MYHB [accession number AAF61445], Bt MYHB [accession number BAA36494], Gg MYHIIB [accession number AAA48988], Xl MYHB [accession number AAA49915], Gg SMMHC [accession number P10587], Oc SM2 [accession number P35748], Mm SM2 [accession number JC5421], Dm NMII [accession number AAB09049], and Ce NMYII [accession number AAA83339])

Genome Database, The, http://gdbwww.gdb.org/ (for microsatellite accession numbers)

Online Mendelian Inheritance in Man (OMIM), http://www.ncbi.nlm.nih.gov/Omim/ (for MHA [MIM 155100], FTNS [MIM 153640], SBS [MIM 605249], and EPS and APSM [MIM 153650])

Tandem Repeats Finder, http://c3.biomath.mssm.edu/trf.html

References

Alport AC (1927) Hereditary familial congenital hemorrhagic nephritis. Br Med J 1:504–506

Atkin CL, Gregory MC, Border WA (1986) Alport syndrome. In: Schrier RW, Gottschalk CW (eds) Strauss and Welt's diseases of the kidney. Little Brown, Boston, pp 617–641

Avraham KB, Hasson T, Steel KP, Kingsley DM, Russell LB, Mooseker MS, Copeland NG, Jenkins NA (1995) The mouse Snell's waltzer deafness gene encodes an unconventional myosin required for structural integrity of inner ear hair cells. Nat Genet 11:369–375

Bain BJ (1985) Platelet count and platelet size in males and females. Scand J Haematol 35:77–79

Barker DF, Hostikka SL, Zhou J, Chou LT, Oliphant AR, Gerken SC, Gregory MC, Skilnick MH, Atkin CL, Tryggvason K (1990) Identification of mutations in the COL4A5 collagen gene in Alport syndrome. Science 248:1224–1227

Benson G (1999) Tandem repeat finder: a program to analyze DNA sequences. Nucleic Acids Res 27:573–580

Beohar N, Kawamoto S (1998) Transcriptional regulation of the human nonmuscle myosin II heavy chain-A gene. J Biol Chem 273:9168–9178

Choy YS, Dabora SL, Hall F, Ramesh V, Niida Y, Franz D, Kasprzyk-Obara J, Reeve MP, Kwiatkowski DJ (1999) Superiority of denaturing high performance liquid chromatography over single-stranded conformation and conformation-sensitive gel electrophoresis for mutation detection in TSC2. Ann Hum Genet 63:383–391

Colville D, Wang YY, Jamieson R, Collins F, Hood J, Savige J (2000) Absence of ocular manifestations in autosomal dominant Alport syndrome associated with haematological abnormalties. Opthalmic Genet 21:217–225

Dominguez R, Freyzon Y, Trybus KM, Cohen C (1998) Crystal structure of a vertebrate smooth muscle myosin motor domain and its complex with the essential light chain: visualization of the pre-power stroke state. Cell 94:559–571

Epstein CJ, Sahud MA, Piel CF, Goodman JR (1972) Hereditary macrothromboctopathia, nephritis and deafness. Am J Med 52:299–310

Greinacher A, Bux J, Kiefel V, White JG, Mueller-Eckhardt C (1992) May-Hegglin anomaly: a rare cause of thrombocytopenia. Eur J Pediatr 151:668–671

Greinacher A, Mueller-Eckhardt C (1990*a*) Hereditary types of thrombocytopenia with giant platelets and inclusion bodies in the leukocytes. Blut 60:53–60

Greinacher A, Nieuwenhuis HK, White JG (1990*b*) Sebastian platelet syndrome: A new variant of hereditary macrothrombocytopenia with leukocyte inclusions. Blut 61:282–288

Harrington WF, Rodgers ME (1984) Myosin. Annu Rev Biochem 53:35–73

Hegglin R (1945) Gleichzeitige konstitutionelle Veranderungen an Neurtophilen und Thrombocyten. Helv Med Acta 12: 439–440

Houdusse A, Sweeney HL (2001) Myosin motors: missing structures and hidden springs. Curr Opin Struct Biol 11: 182–194

Jones TA, Zou JY, Cowan SW, Kjeldgaard M (1991) Improved methods for the building of protein models in electron density maps and the location of errors in these models. Acta Crystallogr A 47:110–119

Kawamoto S (1994) Evidence for an internal regulatory region in a human nonmuscle myosin heavy chain gene. J Biol Chem 269:15101–15110

Kelley MJ, Jawien W, Ortel TL, Korczak JF (2000) Mutation of MYH9, encoding non-muscle myosin heavy chain A, in May-Hegglin anomaly. Nat Genet 26:106–108

Kunishima S, Kojima T, Matsushita T, Tanaka T, Tsurusawa M, Furukawa Y, Nakamura Y, Okamura T, Amemiya N, Nakayama T, Kamiya T, Saito H (2001) Mutations in the NMMHC-A gene cause autosomal dominant macrothrombocytopenia with leukocyte inclusions (May-Hegglin anomaly/Sebastian syndrome). Blood 97:1147–1149

Lalwani AK, Goldstein JA, Kelley MJ, Luxford W, Castelein CM, Mhatre AN (2000) Human nonsyndromic hereditary deafness DFNA17 is due to a mutation in nonmuscle myosin *MYH9*. Am J Hum Genet 67:1121–1128

Liu XZ, Walsh J, Mburu P, Kendrick-Jones J, Cope MJ, Steel KP, Brown SD (1997) Mutations in the myosin VIIA gene cause non-syndromic recessive deafness. Nat Genet 16:188–190

Lu RC, Wong A (1989) Glutamic acid-88 is close to SH-1 in the tertiary structure of myosin subfragment 1. Biochemistry 28:4826–4829

Martignetti JA, Heath KE, Harris J, Bizzaro N, Savoia A, Balduini CL, Desnick RJ (2000) The gene for May-Hegglin anomaly localizes to a <1-Mb region on chromosome 22q12.3-13.1. Am J Hum Genet 66:1449–1454

May R (1909) Leukocyteneinschlusse. Deutsch Arch Klin Med 96:1–6

May-Hegglin/Fechtner Syndrome Consortium (2000) Mutations in *MYH9* result in May-Hegglin anomaly, Fechtner and Sebastian syndromes. Nat Genet 26:103–105

Melchionda S, Ahituv N, Bisceglia L, Sobe T, Glaser F, Rabionet R, Arbones ML, Notarangelo A, Di Iorio E, Carella M, Zelante L, Estivill X, Avraham KB, Gasparini P (2001) *MYO6,* the human homologue of the gene responsible for deafness in *snell's waltzer* mice, is mutated in autosomal dominant nonsyndromic hearing loss. Am J Hum Genet 69: 635–640

Mhawech P, Saleem A (2000) Inherited giant platelet disorders. Classification and literature review. Am J Clin Pathol 113: 176–190

Moxey-Mims MM, Young G, Silverman A, Selby DM, White JG, Kher KK (1999) End-stage renal disease in two pediatric patients with Fechtner syndrome. Pediatr Nephrol 13:782–786

Nadeau JH (2001) Modifier genes in mice and humans. Nat Rev Genet 2:165–174

Nicolaides NC, Stoeckert CJ (1990) A simple, efficient method for the separate isolation of RNA and DNA from the same cells. Biotechniques 8:154–156

Nurden P, Nurden A (1996) Giant platelets, megakaryocytes and the expression of glycoprotein Ib-IX complexes. C R Acad Sci III 319:717–726

O'Neil KT, DeGrado WF (1990) A thermodynamic scale for the helix forming tendencies of the commonly occurring amino acids. Science 250:646–651

Peterson LC, Rao KV, Crosson JT, White JG (1985) Fechtner syndrome— a variant of Alport's syndrome with leukocyte inclusions and macrothrombocytopenia. Blood 65:397–406

Rocca B, Laghi F, Zini G, Maggiano N, Landolfi R (1993) Fechtner syndrome: report of a third family and literature review. Br J Haematol 85:423–426

Schiffer M, Edmundson AB (1967) Use of helical wheels to represent the structures of proteins and to identify segments with helical potential. Biophys J 7:121–135

Sellers JR (1999) Myosins. Oxford University Press, Oxford

——— (2000) Myosins: a diverse superfamily. Biochim Biophys Acta 1496:3–22

Simons M, Wang M, McBride W, Kawamoto S, Yamakawa K, Gdula D, Adelstein RS, Weir L (1991) Human nonmuscle myosin heavy chains are encoded by two genes located on different chromosomes. Circ Res 69:530–539

Tiepold M, Kliche W, Pfannstiel J, Faulstich H (2000) Stepwise modulation of ATPase activity, nucleotide trapping, and sliding motility of myosin S1 by modification of the thiol region with residues of increasing size. Biochemistry 39:1305–1315

Toothaker LE, Gonzalez DA, Tung N, Lemons RS, Le Beau MM, Arnaourt MA, Clayton LK, Tenen DG (1991) Cellular myosin heavy chain in human leukocytes: isolation of 5′ cDNA clones, characterization of the protein, chromosomal localization and upregulation during myeloid differentiation. Blood 78:1826–1833

Toren A, Amariglio N, Rozenfeld-Granot G, Simon AJ, Brok-Simoni F, Pras E, Rechavi G (1999) Genetic linkage of autosomal-dominant Alport syndrome with leukocyte inclusions and macrothrombocytopenia (Fechtner syndrome) to chromosome 22q11-13. Am J Hum Genet 65:1711–1717

Toren A, Rozenfeld-Granot G, Rocca B, Epstein CJ, Amariglio N, Laghi D, Landolfi R, Brok-Simoni F, Carlsson LE, Rechavi G, Greinacher A (2000) Autosomal dominant giant platelet syndromes: a hint of the same genetic defect as in Fechtner syndrome owing to a similar linkage to chromosome 22q11-13. Blood 96: 3447–3451

Velasco F, Espinosa, Torres A (2000) Fechtners syndrome. Haematologica 85:988

Wang A, Liang Y, Fridell RA, Probst FJ, Wilcox ER, Touchman JW, Morton CC, Morell RJ, Noben-Trauth K, Camper SA, Friedman TB (1998) Association of unconventional myosin MYO15 mutations with human nonsyndromic deafness DFNB3. Science 280:1447–1451

Weil D, Blanchard S, Kaplan J, Guilford P, Gibson F, Walsh J, Mburu P, Varela A, Levilliers J, Weston MD, Kelley PM, Kimberling WJ, Wagenaar M, Levi-Acobias F, Larget-Piet D, Munnich A, Steel KP, Brown SDM, Petit C (1995) Defective myosin VIIA gene responsible for Usher syndrome type 1B. Nature 374:60–61

Weil D, Kussel P, Blanchard S, Levy G, Levi-Acobas F, Drira M, Ayadi H, Petit C (1997) The autosomal recessive isolated deafness, DFNB2, and the Usher 1B syndrome are allelic defects of the myosin-VIIA gene. Nat Genet 16:191–193